Shape Measurement of Bubble in a Liquid-Metal

Y. Saito[1*], X. Shen[1], K. Mishima[1], and M. Matsubayashi[2]

[1]Research Reactor Institute, Kyoto University, Osaka, Japan
[2]Tokai Establishment, Japan Atomic Energy Agency, Ibaraki, Japan

Keywords: Neutron radiography, Two-phase flow, Direct contact heat transfer, Bubble shape

Abstract

Dynamic behavior of a two-phase bubble, i.e. a steam bubble containing a droplet evaporating in the bubble, in the molten alloy was clearly visualized by using high-frame rate neutron radiography. In relation to some direct contact heat exchanger design with molten lead-bismuth (Pb-Bi), experiments have been done at JRR-3M of JAEA (Japan Atomic Energy Agency) with water droplets evaporating in a stable thermally stratified Newton's alloy pool. The instantaneous shape and size of the bubble has been iteratively estimated from the void fraction distributions and total void volume by assuming a symmetrical bubble shape.

* Corresponding author. Tel.: +81(72)451-2374; fax: +81(72)451-2620. E-mail address: ysaito@rri.kyoto-u.ac.jp (Y. Saito).

1. Introduction

Direct contact heat exchanger between dispersed droplets and an immiscible liquid has been attractive industrial applications due to its high heat transfer efficiency. Because of the absence of solid walls between the fluids, the process has many advantages compared to conventional heat exchangers. Those advantages have stimulated research on its utilization for liquid metal cooled nuclear power plants (Kinoshita, 1995, Buongiorno et al., 2001, Uchida et al., 2005, Takahashi et al., 2005). In such a reactor, water is injected into heated molten metal and direct boiling of water droplets takes place.

So far numerous studies have been already reported on the direct contact heat transfer (Sidemann, 1966, Tochitani 1977, Simpson et al. 1974), however such studies were been performed with aqueous solutions and hydrocarbons (freon, butane, pentane). Little is available with a molten alloy. Kinoshita et al. (1995) reported experimental results for boiling of water in a Pb-Bi pool. Nishi et al. (1996, 1998) visualized boiling of water in Newton's alloy (solder #95) by using neutron radiography. They measured the rising velocity of two-phase bubbles in a molten alloy and the interfacial heat transfer coefficients. Abdulla et al. (2002) visualized boiling of water in Pb-Bi by using the X-ray imaging method and measured the overall volumetric heat transfer coefficient. The present authors have performed heat transfer experiments by using neutron radiography to obtain the rising velocity and heat transfer coefficient of two-phase bubble. The obtained bubble images suffered from statistical noise in counting neutrons, then the equivalent spherical diameter have been calculated from area averaged void fractions, even though cap-shaped or ellipsoidal bubbles were observed during the evaporation process.

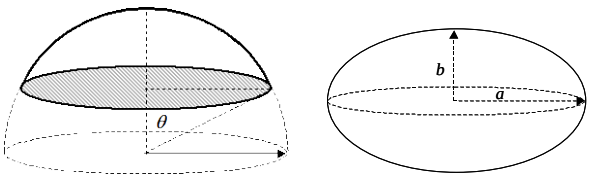

Fig. 1. Axial symmetrical bubble.

The purpose of this study is to determine the shape and size of the boiling two-phase bubble by using high-frame rate neutron radiography and to measure the rising velocities, interfacial area, and interfacial heat transfer coefficients. Theoretically it is of course impossible to determine three dimensional bubble shape by using one projection image. Even so we encounter often situations where the outline can be assumed. The shape of rising bubble may change smoothly from spherical to cap shape. Thus, by assuming the axial symmetry bubble shape and size are estimated Calculation procedure and the evaporating behavior are clarified in this study.

2 Experiments

2.1 Neutron radiography

Figure 2 illustrates the basic concept of dynamic neutron radiography. After the penetrated neutron beam is changed into visible light by a converter, it is detected by a high sensitivity imaging system. A high-speed video camera (Photron, Super 10K) combined with an image intensifier (Hamamatsu, C6598-50MOD) (Saito et al., 2005) was used to take the light intensity of phosphorescent images on a fluorescent converter. The Japan Research Reactor 3 Modified (JRR-3M) of the Japan Atomic Energy Agency (JAEA) was used as a neutron source in this study. Images of multiphase flow were taken by high frame rate neutron radiography at 250frames/s.

2.2 Experimental apparatus

Figure 3 shows the schematic of the test section. The test section was a rectangular tank made of aluminum plates with 5 mm thickness (400mm height and $80\times30mm^2$). A stainless steel nozzle (0.5 mm inner diameter) was mounted at the bottom of the tank. The upper part of the tank was heated by electric heaters and the aluminum fin block connected to the bottom part was cooled by a DC cooling fan to realize stable thermal stratification. Distilled water was used for the dispersed phase and Newton's alloy was chosen for the continuous phase. The properties of Newton's alloy and Pb-Bi are shown in Table 1. The test section was filled with Newton's alloy and the initial depth was 25cm. Six sheathed thermocouples were installed to measure the temperature distributions in the continuous phase. Experiments were carried out by varying the temperature gradient in the continuous phase as shown in Table 2. Water flow rate was 7.64×10^{-3} g/s and the initial diameter of water droplet was 3.6mm.

3. Analysis

At first the void/water fraction around evaporating bubble was calculated (Please see Saito et al. 2006). However, such measured fraction would suffer from severe statistical noise. It would be difficult to determine the actual bubble shape by applying simply image binarization.

Generally a rising bubble will change from spherical to cap shape and keep smooth interface. If we can assume axial symmetry of the bubble shape, the shape and size of bubbles could be determined from noisy neutron images.

Table 1 Properties of Newton's alloy.

Compositions [wt%]	Bi-Pb-Sn 50.0-31.2-18.8
Melting point [°C]	94
Density	9490*
Thermal conductivity [W/mK]	13.5*
Macroscopic cross section [cm-1]	0.274*

* estimated value

Table 2 Experimental conditions.

Run No.	TC1 [°C]	TC2 [°C]	TC3 [°C]	TC4 [°C]	TC5 [°C]	TC6 [°C]	Temperature Gradient $(\Delta T/\Delta y)_{ave}$ [K/m]	Comments
Run 4	104.4	105.8	106.2	106.1	103.7	100.1	25	Non boiling
Run 5	107.4	109.0	108.2	107.2	104.2	100.2	40	Non boiling
Run 6	111.2	111.7	110.3	107.5	103.9	100.0	64.5	Non boiling
Run 7	115.3	115.3	112.0	108.5	104.0	100.0	80.5	Boiling
Run 8	120.2	118.7	115.3	110.0	104.5	100.0	107.5	Boiling
Run 9	125.0	124.3	119.6	112.2	105.3	100.6	142.5	Boiling
Run 10	125.0	125.2	124.7	121.7	111.0	102.0	137	Boiling
Run 11	130.2	129.6	128.8	121.8	109.9	102.4	188.5	Boiling
Run 12	134.8	134.7	133.7	129.5	111.4	101.8	223	Boiling
Run 13	140.5	140.2	139.1	136.2	115.2	101.4	239	Boiling
Run 14	144.1	144.0	143.0	138.2	121.6	104.1	213.5	Boiling

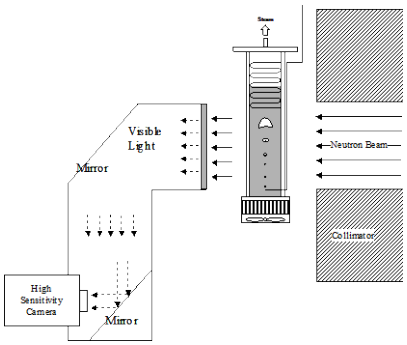

Fig. 2. Dynamic neutron radiography.

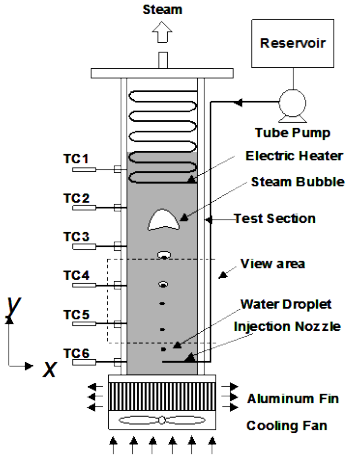

Fig. 3. Schematic of the test section.

Let us consider the integration of local void fraction in a reference area. From the mass balance of a water droplet in a single two-phase bubble, the following relationship can be obtained:

$$\iint \left(\rho_V \delta_V + \rho_W \delta_W\right) dxdy = const. \tag{1}$$

where δ denotes the thickness of the object. The subscripts *V* and *W* denote vapor and water, respectively. Thus, the volume of the two-phase bubble can be expressed as follows:

$$\begin{aligned} V &= \delta_L \iint \left(\alpha_V + \alpha_W\right) dxdy \\ &= \delta_L \iint \left(ln\left(\frac{G_L - G_0}{G_{MP} - G_0}\right) \Big/ ln\left(\frac{G_L - G_0}{G_G - G_0}\right)\right) dxdy \\ &\quad + \frac{\Sigma_W}{\Sigma_{LM}} \frac{1}{\rho_W} \iint \left(\rho_W \delta_W + \rho_V \delta_V\right) dxdy \end{aligned} \tag{2}$$

where, α_V is the void fraction and α_W is the water fraction, respectively. The subscripts *L*, *G*, *MP*, and *LM* denote liquid single phase, gas single phase, multiphase mixture and Liquid-metal, respectively. G_0 is the offset term of the gray level. In addition, the initial volume of the water droplet, V_{ini} can be expressed from the images in non-boiling region:

$$V_{ini} = \frac{\delta_L \iint \left(ln\left(\frac{G_L - G_0}{G_{MP} - G_0}\right) \Big/ ln\left(\frac{G_L - G_0}{G_G - G_0}\right)\right) dxdy}{\left(1 - \Sigma_W / \Sigma_{LM}\right)} \tag{3}$$

Therefore, the volume of the two-phase bubble can be calculated from the following equation:

$$V = \delta_L \iint \left(ln\left(\frac{G_L - G_0}{G_{MP} - G_0}\right) \Big/ ln\left(\frac{G_L - G_0}{G_G - G_0}\right)\right) dxdy + \frac{\Sigma_W}{\Sigma_{LM}} V_{ini} \tag{4}$$

The equivalent diameter D_e can be calculated by:

$$D_e = \sqrt[3]{\frac{6V}{\pi}} \tag{5}$$

Figure 4 shows the schematic of the calculation of the bubble aspect ratio *H/W*. The vertical symmetry H_{upper}/H_{down} can be also calculated. If the vertical symmetry is larger than a certain value c_1 (=1.2), the bubble changes from ellipsoidal to cap shape as shown in Fig.5. The major axis *a* and minor axis *b* of ellipsoidal bubble, and the curvature *R* and the open angle of cap bubbles can be determined by using the following equations.

For ellipsoidal bubble:

$$a = \sqrt[3]{H/W}\, D_e / 2 \tag{6}$$

$$b = \left(H/W\right)^{-2/3} D_e / 2 \tag{7}$$

For cap bubble:

$$cos\,\theta = \left(\left(H/W\right)^2 - 4\right) \Big/ \left(\left(H/W\right)^2 + 4\right) \tag{8}$$

$$R = D_e \Big/ \sqrt[3]{4 - 6\cos\theta + 2\cos^3\theta} \tag{9}$$

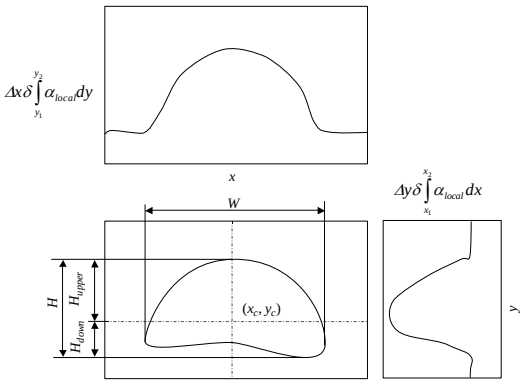

Fig. 4. Calculation of aspect ratio and vertical symmetry.

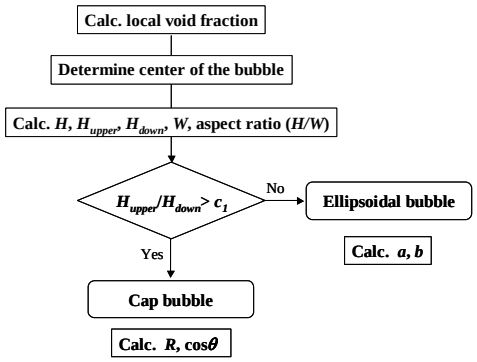

Fig. 5. Determination of bubble shape.

4 Results and discussions

4.1 Bubble shape determination

Figure 6 shows examples of processed images. Figure 6(a) was obtained by simple image binarization. The bubble shapes show jagged interface due to image noise. Figure 6(b) shows calculated bubble shape superimposed on original processed images. Figure 6(c) shows the calculated bubble shape. As shown in these figures the calculated bubble shape and size agree well with the visualization results. The sloshing behavior of water droplets could not be clearly observed in the static images. It should be noted here that the oscillation causes a liquid film to form on the internal surface of the envelope, thus increasing the liquid-liquid surface area and heat transfer coefficient (Simpson et al., 1974).

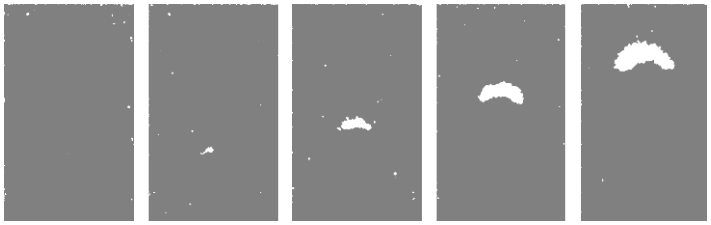

Fig. 6(a) Simple image binarization.

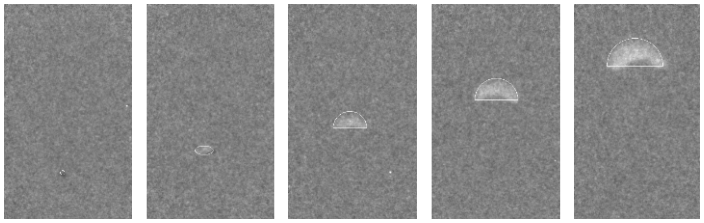

Fig. 6(b) Original bubble image and calculated results.

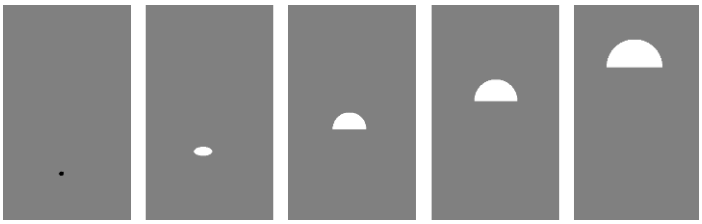

Fig. 6(c) Calculated bubble shape.

Fig. 6. Consecutive bubble images.

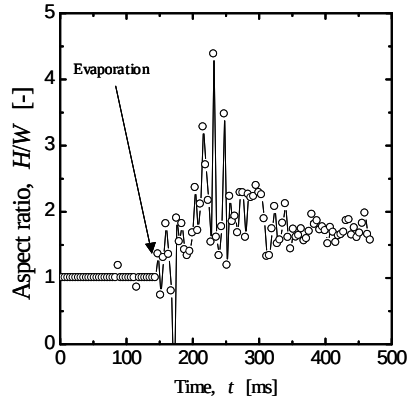

Fig. 7. Calculated bubble aspect ratio.

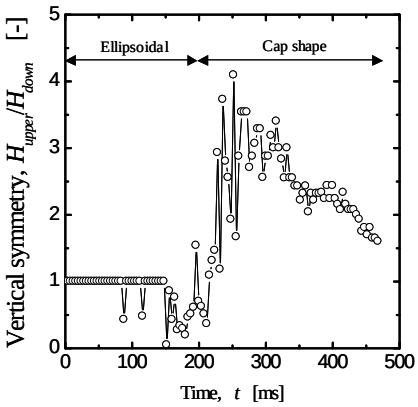

Fig.8. Vertical symmetry of bubble.

4.2 Dynamic behavior of two-phase bubble

Figures 7 and 8 denote the bubble aspect ratio and vertical symmetry, respectively. At t =150ms the water droplet begins to evaporate and the aspect ratio increases gradually at first. The vertical symmetry decreases after 300ms. The convex bottom shape of the cap bubble may result in the decreasing tendency. Visualization results indicate that the bubble shape stays ellipsoidal at t =150-220ms and then changes into cap shape. It can be seen from this figure that the aspect ratio increases rapidly at t =220-250ms. This may be caused by the sloshing of water droplets inside the bubble. However, at the present study it is still difficult to discriminate water droplets from gas phase. Further study should be required to make clear the droplets behavior.

5.Conclusions

Direct contact evaporation of a water droplet in a molten metal pool has been visualized by using high-frame rate neutron radiography. The conclusions obtained are as follows:

1) Direct contact evaporation phenomena was clearly visualized.
2) By assuming axial symmetry bubble shape and size were determined. Calculated results indicate that this symmetrical assumption is still acceptable at the present experimental conditions.
3) Two-phase bubble expands rapidly in the lateral direction at the transition from ellipsoidal to cap shape.

References

[1] S.Abdulla et al., Heat Transfer 2002, Proc. 12th IHTC, (2002)Grenoble, France
[2] J.Buongiorno et al., ICONE-9772, Proc. 9th Int. Conf. Nuclear Engineering (2001) Nice, France, April 8-12
[3] I.Kinoshita et al., Proc. 3rd JSME/ASME Joint Int. Conf. Nuclear Engineering (1995) Kyoto, Japan
[4] Y.Nishi et al., Komae Research Laboratory Rep. No.T95061 (1996) (in Japanese)
[5] Y.Nishi et al., Proc. 11th IHTC, Kyongju, Korea, (1998) August 23-28
[6] Y. Saito et al., Nucl. Instr. and Meth., 542 (2005) 309
[7] S.Sideman, J.Isenberg, Desalination, 2 (1967) 207
[8] S.Sideman, Y.Taitel, Int. J. Heat Mass Transfer, 7 (1964) 1273
[9] HC.Shimson et al., Heat Transfer 5, (1974) 59